Supporting Materials

Photoluminescence Enhancement and Structure Repairing of Monolayer $MoSe_2$ by Hydrohalic Acid Treatment

Hau-Vei Han,[¶,#,†] Ang-Yu Lu,[#,†] Li-Syuan Lu,[§] Jing-Kai Huang,[#] Henan Li,[#] Chang-Lung Hsu,[‡] Yung-Chang Lin,[&] Ming-Hui Chiu,[#] Kazu Suenaga,[&] Chih-Wei Chu,[‡] Hao-Chung Kuo,[¶*] Wen-Hao Chang,[§,||] Lain-Jong Li[#,*] and Yumeng Shi[#,*]

[#]*Physical Sciences and Engineering Division, King Abdullah University of Science and Technology, Thuwal, 23955-6900*

[¶] *Department of Photonics and Institute of Electro-Optical Engineering, National Chiao Tung University, Hsinchu, Taiwan*

[§] *Department of Electrophysics, National Chiao Tung University, Hsinchu, Taiwan.*

[||] *Taiwan Consortium of Emergent Crystalline Materials (TCECM), Ministry of Science and Technology, Taiwan.*

[‡] *Research Center for Applied Sciences, 128 Sec. 2, Academia Rd., Nankang, Taipei 11529, Taiwan*

[&] *National Institute of Advanced Industrial Science and Technology (AIST), Tsukuba, Japan*

[*]To whom correspondence should be addressed: (H.C. Kuo) hckuo@faculty.nctu.edu.tw; (L. J. Li) lance.li@kaust.edu.sa; (Y. Shi) yumeng.shi@kaust.edu.sa

† These authors contribute equally

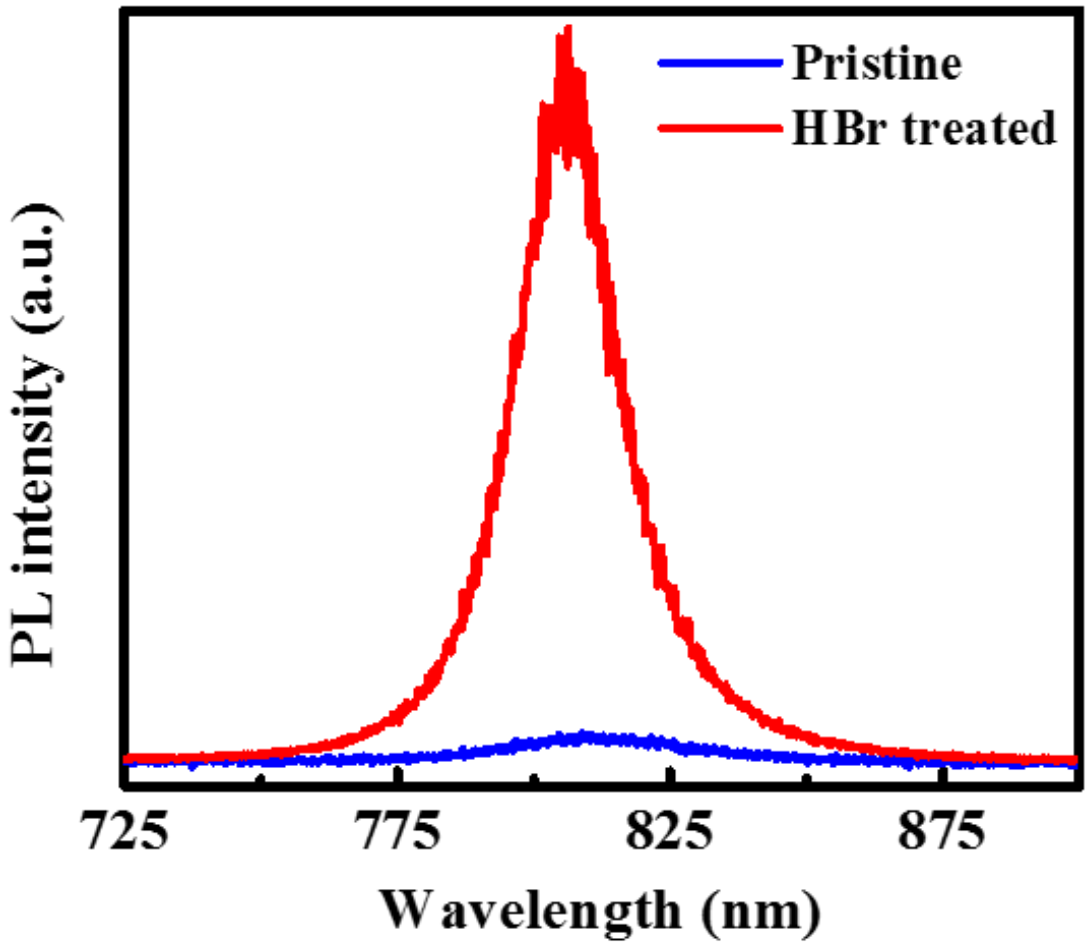

Figure S1. PL spectrum of as-grown and HBr treated $MoSe_2$ monolayer at room temperature.

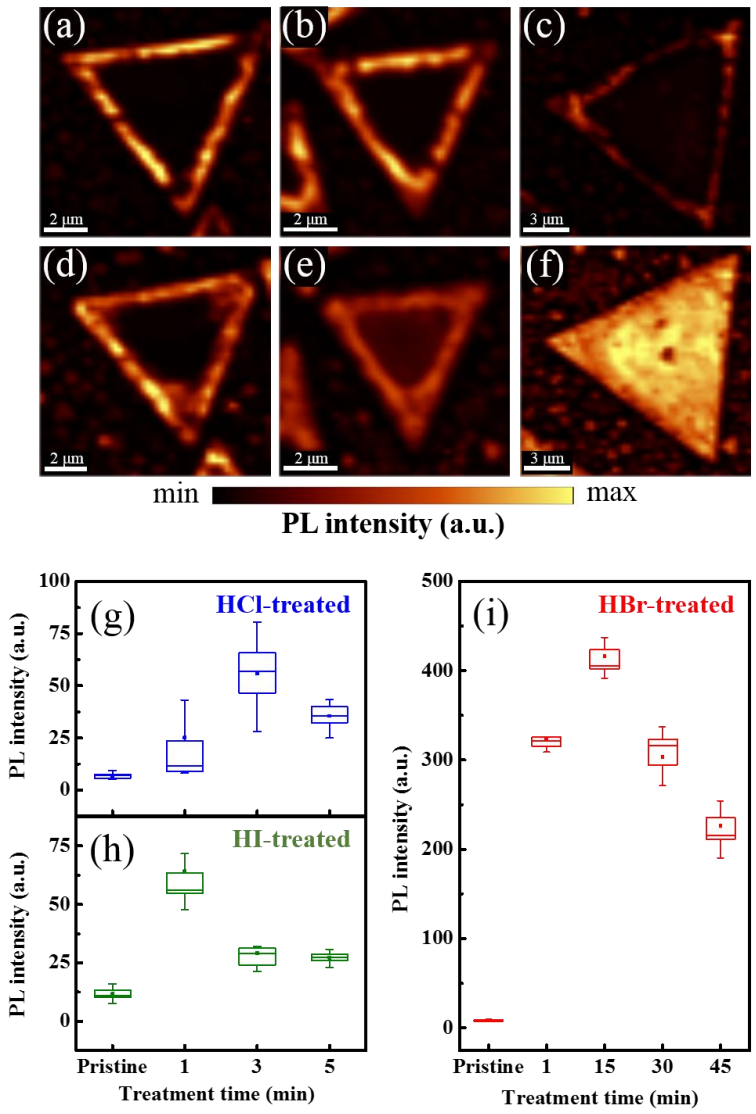

Figure S2. **(a)**, **(b)** and **(c)** show three PL intensity maps of as-grown $MoSe_2$ layers used for HCl, HI and HBr treatment. The corresponding PL intensity maps after chemical treatment are displayed in **(d)**, **(e)** and **(f)** respectively. **(g)**, **(h)** and **(i)** show the time dependence of PL intensity changes upon HCl, HI and HBr treatment. Noted that we have performed each treatment for different time periods. The HCl treatment can only slightly enhance the PL intensity while for HI the $MoSe_2$ layers shows an increase in PL intensity followed by a fast PL weakening which could be due the corrosion by the strong acidic nature.

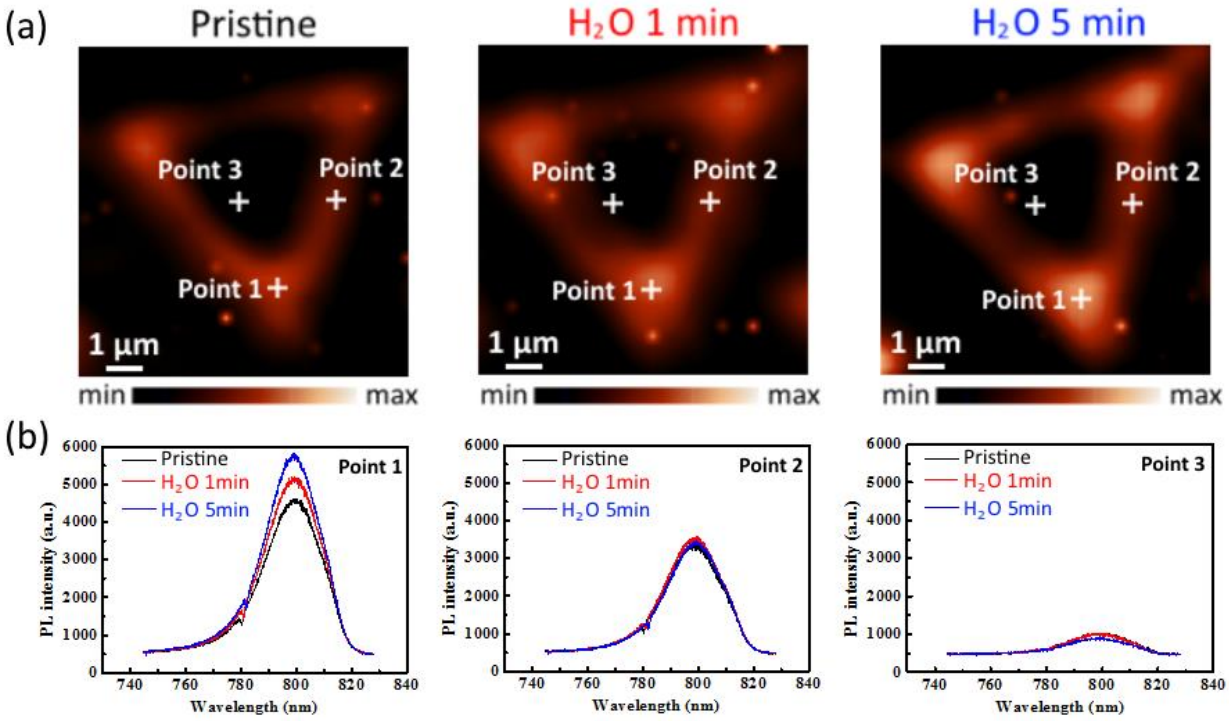

Figure S3. (a) The PL intensity mappings of an individual $MoSe_2$ flake before and after H_2O treatment for 1 minute and 5 minutes respectively; **(b)** PL intensity comparison at different surface locations as indicated in Figure **(a).**

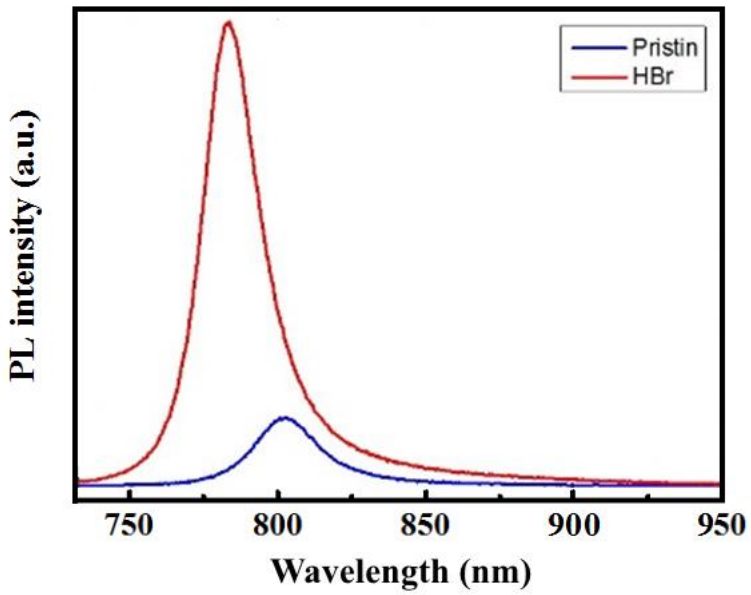

Figure S4. PL comparison of pristine and HBr treated $MoSe_2$ monolayer in vacuum condition at a pressure of 4×10^{-3} Torr. By comparing the PL intensity change for the sample before and after HBr treatment in vacuum, we exclude other possible gaseous adsorption effects (for example, moisture and O_2) on the optical properties.

The calculation of carrier density

In $MoSe_2$, the exciton and trion peak position follow the equation of standard temperature bandgap dependence [1]

$$E_g(T) = E_g(0) - S\hbar\omega[\coth\left({}^{\hbar\omega}/_{2k_BT}\right) - 1] \quad \text{eq (1)}$$

where $E_g(0)$ is the ground-state transition energy at 0 K, S is a dimensionless coupling constant and $\hbar\omega$ is an average phonon energy. From the PL measurement at low temperature, the photon energy of exciton (X^0) and trion (X^-) can be determined for 1.66 eV and 1.63 eV, respectively. The dimensionless coupling constant of exciton (X^0) and trion (X^-) are set to 1.96 and 2.24 according to the previously reported.[2] Therefore, the calculated photon energy of exciton and trion at 300 K are 1.58 eV and 1.54 eV, as shown in **Figure S5**.

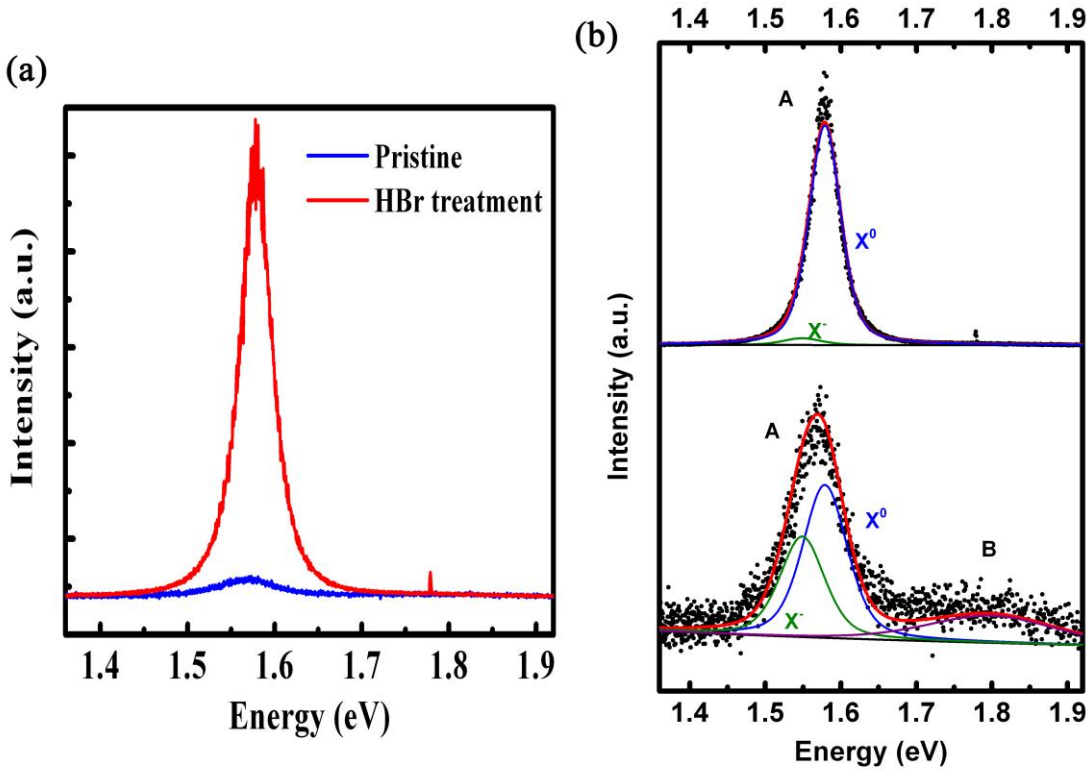

Figure S5. (a) $MoSe_2$ PL before and after HBr treatement at room temeparture; (b) coresponding trion and exciton peak fitting for HBr treated (upper) and pristine (lower) $MoSe_2$.

The PL intensity of the exciton (I_X) and trion (I_{X^-}) are related to their populations which can be expressed as :

$$I_X \approx \frac{G\gamma_{ex}}{k_{tr}} \qquad \text{eq(2)}$$

$$I_{X^-} \approx \frac{G\gamma_{tr}}{\Gamma_{tr}} \qquad \text{eq(3)}$$

where, G is the optical generation rate of exciton, $k_{tr}(t)$ is the formation rate of the trion from the exciton and Γ_{tr} is the decay rate of the trion. Based on the previous work [3], the radiative decay rate of exciton (γ_{ex}) and trion (γ_{tr}) are 3 ps^{-1} and 12 $ps^{-1,}$ respectively.

The electron density in single-layered $MoSe_2$ follows the mass action law relating the electron density (n_{el}), concentration of exciton (N_x) and trion (N_{x^-})[4].

$$\frac{N_X\, n_{el}}{N_{X^-}} = \left(\frac{4m_X m_e}{\pi\hbar m_{X^-}}\right) k_B T exp\left(-\frac{E_b}{k_B T}\right) \qquad \text{eq(4)}$$

where T is the temperature, k_B is Boltzmann constant, E_b is the trion binding energy and m_X and m_{X^-} is the effective masses of an exciton and trion, respectively. Here $\left(\frac{4m_X m_e}{\pi\hbar m_{X^-}}\right)$ is $6.18 \times 10^{11}\, cm^{-2} \cdot meV$ by using a reported data[2]. Combining the eq (2), (3) and (4), the electron density can be estimated from the trion PL intensity as the equation:

$$\frac{I_{X^-}}{I_{total}} = \frac{\frac{\gamma_{tr}}{\gamma_{ex}}\frac{N_{X^-}}{N_x}}{1+\frac{\gamma_{tr}}{\gamma_{ex}}\frac{N_{X^-}}{N_x}} \approx \frac{8\times10^{-13} n_{el}}{1+8\times10^{-13} n_{el}}$$

Adapting the PL intensity fitting results from **Figure S5b**, the electron carrier can be estimated to be 8.2 × 10^{11} cm^{-2} for as-grown and 6.37×10^{10} cm^{-2} for HBr treated $MoSe_2$ respectively, which are within a comparable range with the previous report [2].

Supplemental Reference:

1. O'Donnell, K. P.; Chen, X., Temperature Dependence of Semiconductor Band Gaps. *Appl. Phys. Lett.* 1991, 58, 2924-2926.
2. Ross, J. S.; Wu, S.; Yu, H.; Ghimire, N. J.; Jones, A. M.; Aivazian, G.; Yan, J.; Mandrus, D. G.; Xiao, D.; Yao, W.; Xu, X., Electrical Control of Neutral and Charged Excitons in a Monolayer Semiconductor. *Nat. Commun.* 2013, 4, 1474.
3. Wang, G.; Palleau, E.; Amand, T.; Tongay, S.; Marie, X.; Urbaszek, B., Polarization and Time-resolved Photoluminescence Spectroscopy of Excitons in $MoSe_2$ Monolayers. *Appl. Phys. Lett.* 2015, 106, 112101.
4. Mouri, S.; Miyauchi, Y.; Matsuda, K., Tunable Photoluminescence of Monolayer MoS_2 via Chemical Doping. *Nano Lette.* 2013, 13, 5944-5948.

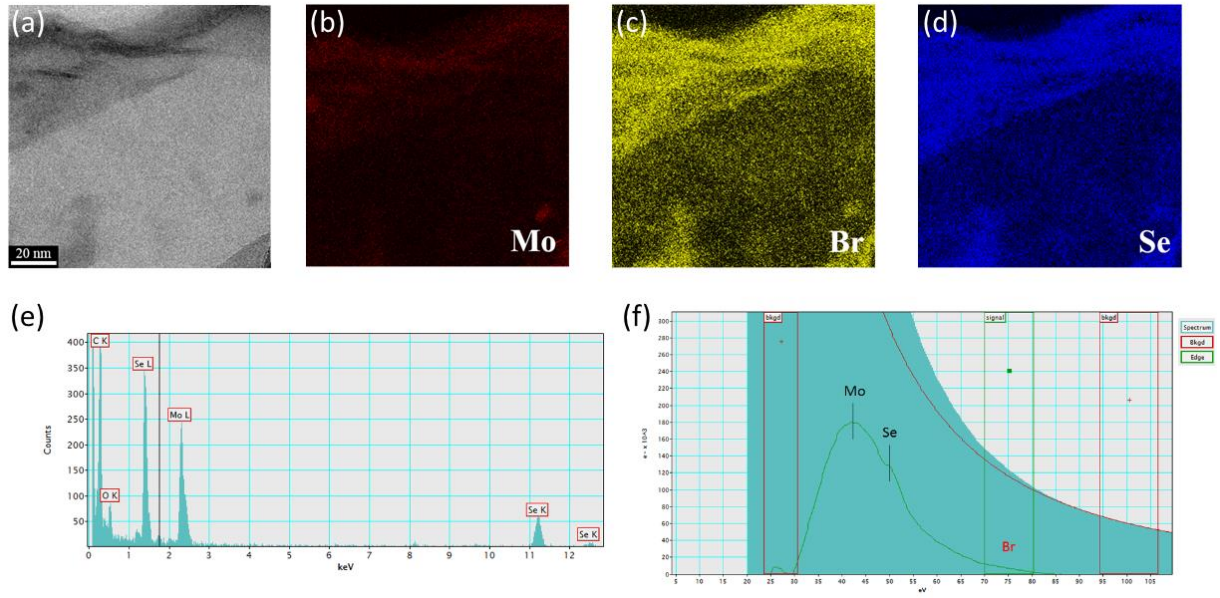

Figure S6. (a) Low magnification TEM image of monolayer $MoSe_2$ with folded edges (darker color) after HBr treatment. **(b)**, **(c)** and **(d)** shows the electron energy loss spectrum (EELS) map of Mo, Br and Se. **(e)** shows an energy-dispersive X-ray spectroscopy (EDS) of $MoSe_2$ monolayer, where Mo and Se can be identified. **(f)** display a typical EELS spectrum of HBr treated $MoSe_2$ monolayer.

In our sample transfer process (see Method section), several chemicals including Poly(methyl methacrylate) (PMMA), diluted-Hydrogen fluoride, deionized (DI) water, Chloroform, Acetone, and Isopropyl alcohol (IPA) were subsequently used. The Br containing group may be effectively removed during transfer process. Also the chemical residuals from transfer process could also cover the sample surface and hinder the investigation of the atomic structure and chemical composition. Therefore, in order to have a clue for the distribution of Br containing group on $MoSe_2$ surface, and limit the interruption from transfer process. We utilized a PMMA-free transfer method for TEM characterization, where scratching the sample surface with sharps and gently resining with DI water were applied. The exfoliated samples can be carried on TEM grids by the DI water droplet. Although Br signal is not strong enough to be detected by EDS as shown in Figure S6 (e), in EELS spectrum a small hump with intensity slightly higher than the background appears within the Br energy region. Energy filtered EELTS map shown in Figure S6 (c) which suggest the possible Br distribution on sample surface.

XPS fitting analysis:

In brief, the peaks in each Mo, Se and Br doublet should have the same FWHM, and the peak area ratio in each doublet is assigned based on the degeneracy of the spin state.

Several criteria are used for the fitting:

(1) The peaks have specific area ratios based on the degeneracy of spin state (see Table R1)
$j = l + s$ (j: spin state, l: angular momentum quantum, s: spin angular momentum)

(2) Splitting doublet
Mo $3d_{5/2} – 3d_{3/2}$ doublet separation is ~3.13 eV

Se $3d_{5/2} – 3d_{3/2}$ doublet separation is ~0.86 eV

Br $3d_{5/2} – 3d_{3/2}$ doublet separation is ~1.05 eV

(3) Average Matrix Relative Sensitivity Factors (AMRSFs)

: Al x-rays ratioed to C (see Table R2)

(4) Background fitting: Shirley method

(5) Fitting Curve: 20% Lorentzian-Gaussian (20LG)

Table R1. The peak area ratios of spin-orbit splitting values

Subshell	***j values***	***Area Ratio***
s	1/2	n/a
p	1/2 3/2	1:2
d	3/2 5/2	2:3
f	5/2 7/2	3:4

Table R2. The average matrix relative sensitivity factors (AMRSFs) of molybdenum, sulfur and oxygen ratioed to C as unity for Al X-rays.

AMRSFs (Al X-rays)	***Molybdenum***	***Selenium***	***Bromine***
$3d_{5/2}$	5.82	1.55	1.91
$3d_{3/2}$	4.01	1.07	1.32

Table R3. The XPS fitting results of binding energy for Mo, Se and Br in pristine $MoSe_2$ and HBr treatment MoSe2 including peak position, full width at half maximum (FWHM) and peak area.

	Pristine $MoSe_2$			**HBr treated $MoSe_2$**		
	Position (eV)	**FWHM (eV)**	**Area**	**Position (eV)**	**FWHM (eV)**	**Area**
$Mo^{(IV)}$ $3d_{5/2}$	229.6	1.53	34.26	229.4	1.06	59.1
$Mo^{(IV)}$ $3d_{3/2}$	232.73	1.53	22.84	232.53	1.06	39.4
$Mo^{(VI)}$ $3d_{5/2}$	233.1	3.71	10.38	233.3	2.57	8.46
$Mo^{(VI)}$ $3d_{3/2}$	236.23	3.71	6.92	236.43	2.57	5.64
Se^{2-} $3d_{5/2}$	54.8	0.77	13.62	54.8	0.78	55.38
Se^{2-} $3d_{5/2}$	55.66	0.77	9.08	55.66	0.78	36.92
S_2^{2-} $3d_{3/2}$	55.34	1.5	12.54	55.34	0.56	7.44
S_2^{2-} $3d_{3/2}$	56.2	1.5	8.36	56.2	0.56	4.96
S^0 $3d_{5/2}$	55.9	1.44	18.48			
S^0 $3d_{3/2}$	56.76	1.44	12.32			
SeO_2 $3d_{5/2}$	59.2	2.47	13.2			
SeO_2 $3d_{3/2}$	60.06	2.47	8.8			
Br^{1-} $3d_{5/2}$				68.8	1.08	47.58
Al_2O_3 $2p_{3/2}$	74.4	1.16		74.4	1.22	31.72